

# Estimation of automotive brake drum–shoe interface friction coefficient under varying conditions of longitudinal forces using Simulink

H. P. KHAIRNAR<sup>1,\*</sup>, V. M. PHALLE<sup>2</sup>, S. S. MANTHA<sup>3</sup>

<sup>1</sup> Mechanical Engineering Department, VJTI, Mumbai, India

<sup>2</sup> Mechanical Engineering Department, VJTI, Mumbai, India

<sup>3</sup> All India Council of Technical Education, New Delhi, India

Received: 19 December 2014 / Revised: 27 March 2015 / Accepted: 11 May 2015

© The author(s) 2015. This article is published with open access at Springerlink.com

**Abstract:** The suitable brake torque at the shoe–drum interface is the prerequisite of the active safety control. Estimation of accurate brake torque under varying conditions is predominantly the function of friction coefficient at the shoe–drum interface. The extracted friction coefficient has been used in the antilock braking system (ABS) algorithm to plot the  $\mu$ –slip curve. The longitudinal forces like Coulomb friction force, contact force and actuating forces at the shoe ends are resolved under the equilibrium condition. The computation of the friction coefficient is presented for the symmetric and asymmetric length of the drum shoes to track the variations in the longitudinal forces. The classical mechanics formulae considering friction are simulated using virtual environment in Matlab/Simulink for the distribution of the Coulomb force. The dual air braking system set up operated at the 8 bar pressure is used to acquire data for the input parameters like distance of Coulomb friction force, distance of pivot point, and contact force applied. The evolved estimation algorithm extracted the maximum friction coefficient of 0.7 for the normal force arrangement of the contact force at the symmetric shoe length, while friction coefficient in the range of 0.3–0.7 is obtained at the asymmetric shoe length.

**Keywords:** friction coefficient; Coulomb friction force; drum brakes; contact force.

## 1 Introduction

Today's rapid technological developments in the automobile industry seek to make accurate, better and safer vehicles. The braking system is integral and vital part of the active safety control of automobile vehicles. The drum braking system works on brake actuating mechanism with the help of drum–shoe interface. The actuating force required for the actuation shoes is transmitted by either wheel cylinders or by cam mechanism. Giri [1] reported two types of actuating mechanisms for drum brakes—in the first type the actuating forces on each shoe are equal and

the second type of mechanisms give equal displacement. The performance of braking system plays an important role in the active safety of the vehicle. During braking in automobiles there is a dynamic transfer of (70%) of total weight onto the front wheels of a vehicle with a corresponding decrease at the rear wheels (30%). Consequently there is a redistribution of usable braking torque at the front and rear brakes in a braking maneuver [2]. Hence, the total steering loss can occur when the dynamic friction coefficient is not as per the requirement of vehicle dynamics, and in quest of this a significant attention has been paid by the researchers and brake designers. The braking process is mainly governed by the longitudinal dynamics of vehicle. The dynamics of braking process depends on friction materials, loading and braking

\*Corresponding author: H. P. KHAIRNAR.  
E-mail: hpkhairnar@vjti.org.in

torque, as well as on dimensional parameters of brake, and these factors also affects on friction coefficient ( $\mu$ ). The earlier researcher's [3–5] contribution for the brake shoe–drum interface predominantly discussed regarding the compositions of the friction materials and proved that friction coefficient ( $\mu$ ) at the brake shoe–drum interface has been primarily the function of the material properties.

Blau [3] presented the report on the brake materials and additive functionality and further discussed about the automotive pad formulations to achieve the stable friction coefficient ( $\mu$ ). The various types of composites affect the friction coefficient ( $\mu$ ), as suggested by Li et al. [4], with the help of the friction testing machine testing the composite materials under dry and wet conditions to study the frictional behavior of the braking system. Maleque et al. [5] studied the material selection to improve the brake system performance depending on the friction coefficient ( $\mu$ ), and their research contributed to the development of the composite material. Apart from the material oriented research several investigators [6–8] have focused on the prediction of the contact pressure between the contacting surfaces in the brakes and squeal analysis which is the significant factor for braking performance. Further Burton et al. [9] reported regarding the contacting spots separated by regions where the surfaces are parted and expressed maximum surface pressure and contact spot width as functions of operating parameters and materials properties. Hohmann et al. [7] dealt with the contact analysis of the drum disk brakes using the finite element methods concluding that the turning moment on the axle due to the brake pressure affects the sticking condition. Attempt has been made by Cueva et al. [10], Guha and Roy [11] to formulate the wear situations in the brake to identify the potential contact points and pressure distribution pattern. Li [12] formulated a mathematical model of the factors influencing the brake force and the results showed that brake force and adhesion coefficients are interdependent. Yasuhisa [13] considered normal load, sliding speed, ambient conditions and material to obtain lower friction coefficient measuring the friction and pull-off forces between a metal pin and plate.

The functional dependence of the friction coefficient ( $\mu$ ) upon a large variety of parameters, including sliding speed by Severin and Dorsch [14] and acceleration, critical sliding distance, temperature, normal load, humidity, surface preparation and of course material combination indicated by Berger [15]. The dynamic friction coefficient ranges even more than one under certain conditions as stated by Kowalski et al. [16]. The dynamic friction coefficient between tire and road is dependent on the longitudinal velocity as demonstrated by Vazquez et al. [17]. However efforts have been made to establish the influence of sliding acceleration to improve the friction coefficient prediction during transient operations which concluded that higher the sliding acceleration, higher the friction coefficient. Most of the materials have exhibited nearly linear dependence of the friction coefficient on the pressure contact in the studied ranges [18]. Friction coefficient is also expressed as the function of sliding velocity, force, time and temperature [17–21]. The braking system produces a Coulomb friction force which is a result of the contact forces at the contact of the leading, trailing shoes and the brake drum. This Coulomb friction force is responsible for the brake torque used to decelerate the vehicle [22] and hence it is pertinent to consider its impact.

Though extensive research work have been carried out in the field of automotive braking system regarding the dependency of the friction coefficient ( $\mu$ ) at the brake shoe–drum interface on various parameters like velocity, contact pressure, temperature, and different compositions of materials [23–25] but it did not analyze the effects of the contact force, actuating force and Coulomb friction force on the friction coefficient ( $\mu$ ).

The present investigation encompasses multitude of equations for friction coefficient derived under the equilibrium condition using principles of classical mechanics with friction considering the variations of longitudinal forces described in Sections 2 and 3. The correlation of temperature, contact pressure, friction force and friction coefficient is discussed in Section 4. Effects of the influential factors such as contact force, brake actuating force and Coulomb friction force on the friction coefficient are evaluated. The relationship

between the above listed longitudinal forces and friction coefficient is modeled using the Simulink and the obtained results are compared with virtual Simulink model of the braking system.

## 2 Estimation of friction coefficient ( $\mu$ ) for symmetric shoe length

During braking operation the actuated shoes result in contact forces  $F_1$  and  $F_t$  for the leading and trailing shoes respectively as shown in Fig. 1. The contact forces  $F_1$  and  $F_t$  are normal to the contact surfaces when contact lining is symmetrical [26–28]. The prevailing force arrangement leads to maximum friction coefficient ( $\mu$ ) due to non existence of components of forces. While deriving the equations,  $F_1$  and  $F_t$  were considered at the distance of the inner drum radius ( $r$ ). However the Coulomb friction forces were also considered at the inner drum radius ( $r$ ). The reactions at hinged point “O” of the brake shoes were considered.

All the forces resolved considering the equilibrium of both brake shoes. Also the values of actuating forces  $W_1$  and  $W_t$  were assumed as equal ( $W_1 = W_t$ ). Hinge reactions ( $H_{x1}$  and  $H_{x2}$ ) for the shoes were considered only for the “X” direction and not in “Y” direction due to the direction of the actuating forces  $W_1$  and  $W_t$ .

However the movement of the vehicle was considered in the longitudinal direction only on the ideally horizontal road. The effects of aerodynamic forces are neglected in the present analysis. The Cartesian coordinate system is  $ox-oy-oz$ ; “x” axis is along the direction of the vehicle movement, “y” axis is along

the lateral movement of the vehicle and “z” axis is along the wheel rotation as shown in Fig. 1. The following equations represents the equilibrium of force system as shown in Fig. 1

$$F_t - F_1 + W_1 - W_t + H_{x1} - H_{x2} = 0 \quad (1)$$

$$\mu F_1 - \mu F_t + mg = 0 \quad (2)$$

Solving both the Eqs. (1) and (2) leads to Eq. (3) giving the cumulative effect since the Coulomb friction force is acting vertical, and the friction coefficient can be estimated using the following equation

$$\mu = \frac{F_t - F_1 + H_{x1} - H_{x2} - mg}{F_1 - F_t} \quad (3)$$

The leading shoe is subjected to dynamic weight transfer resulting in reaction from the contact forces, however moments of contact forces considered at the hinge “O” represent the following equation

$$F_1 h - W_1 r = \mu F_1 h \quad (4)$$

$$\mu = \frac{F_1 h - W_1 r}{F_1 h} \quad (5)$$

For balancing the forces  $F_t$ ,  $W_1$  and  $\mu F_1$  the moments of trailing shoe at the hinge “o” gives the Eq. (5) establishing the effect of “ $F_t$ ”

$$\mu F_t h = W_t r - F_t h \quad (6)$$

$$\mu = \frac{W_t r - F_t h}{F_t h} \quad (7)$$

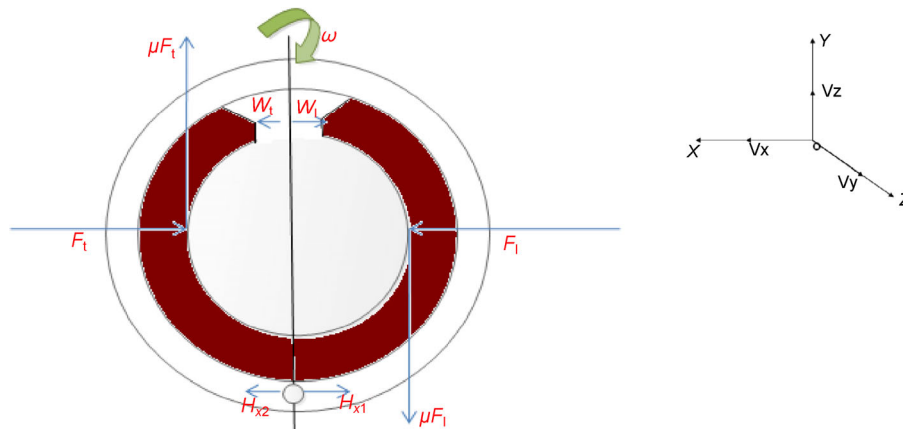


Fig. 1 Equilibrium diagram for the drum brake when contact force is normal.

### 3 Formulation of friction coefficient ( $\mu$ ) for asymmetric shoe length

The methodology for the estimation of friction coefficient ( $\mu$ ) considering variations in  $F_1$  and  $F_t$  at the contact point of the lining-drum is presented below. The friction coefficient ( $\mu$ ) is defined through forces involved in the braking process. Figure 2 shows the arrangement of longitudinal forces  $F_1$  and  $F_t$  in inclined position at the lining-drum contact. The resolution of the forces is shown in the Figs. 3 and 4, considering components of  $F_1$ ,  $F_t$  and Coulomb friction force ( $\mu F_1$  and  $\mu F_t$ ).

The force analysis considering the contact forces ( $F_1$  and  $F_t$ ), actuating forces ( $W_1$  and  $W_t$ ) and hinge reactions ( $H_{x1}$  and  $H_{x2}$ ) is proposed below. The equilibrium condition of the leading shoe and trailing shoe in the

inclined arrangement of  $F_1$  and  $F_t$  is described in the following equations

$$\mu F_1(d - h \cos \theta) = F_1 h \sin \theta - W_1 r \quad (8)$$

$$\mu F_t h = W_t r - F_t h \mu F_1(d - h \cos \theta) = F_1 h \sin \theta - W_1 r \quad (9)$$

$$F_1 \sin \theta - F_t \sin \theta + W_1 - W_t + \mu F_1 \sin \theta + \mu F_t \sin \theta + H_{x1} - H_{x2} = 0 \quad (10)$$

$$F_1 \cos \theta + F_t \cos \theta - \mu F_1 \cos \theta + \mu F_t \cos \theta + mg = 0 \quad (11)$$

Equations (8), (9), (10), (11) are further solved to express the friction coefficient as a function of contact forces ( $F_1$  and  $F_t$ ), actuating forces ( $W_1$  and  $W_t$ ) and distance of Coulomb friction force ( $d$ ).

$$\mu = \frac{-(F_1 - F_t) \sin \theta - H_{x1} + H_{x2}}{(F_1 + F_t) \sin \theta} \quad (12)$$

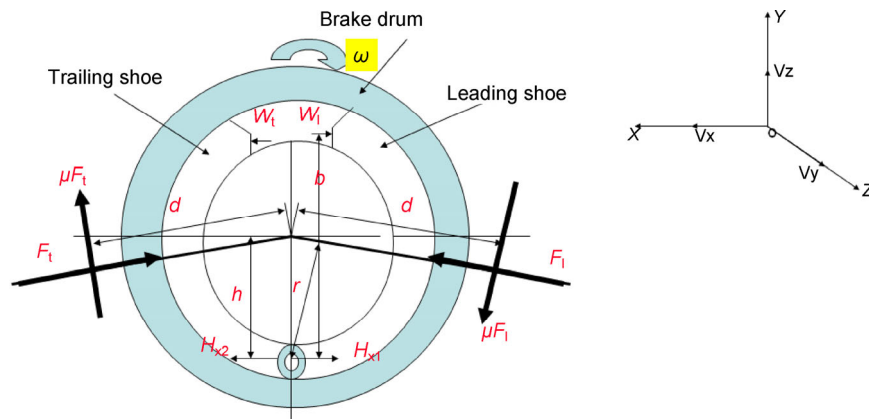


Fig. 2 Equilibrium diagram for the drum brake when contact force is inclined.

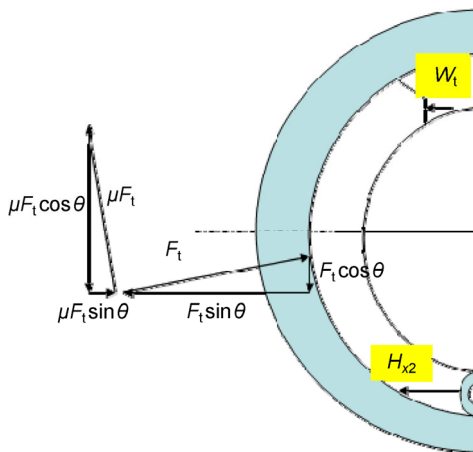


Fig. 3 Forces on trailing shoe.

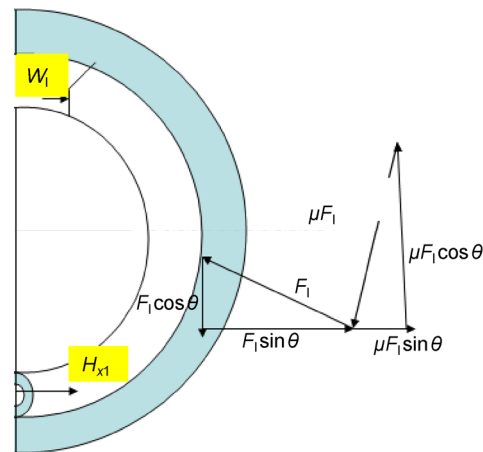


Fig. 4 Forces on leading shoe.

$$\mu = \frac{-(F_1 + F_t) \cos \theta - mg}{(F_t - F_1) \cos \theta} \quad (13)$$

$$\mu = \frac{F_1 h \sin \theta - W_t r}{F_t (d - h \cos \theta)} \quad (14)$$

$$\mu = \frac{W_t r - F_t h \sin \theta}{F_t (d - h \cos \theta)} \quad (15)$$

The magnitude of the friction coefficient ( $\mu$ ) can be computed from the above deduced Eqs. (12), (13), (14) and (15) which is further used in the estimation algorithm. The deduced equations presents database of computed values of the friction coefficient ( $\mu$ ) for the asymmetric shoe length.

#### 4 Friction coefficient with temperature and contact pressure

The temperature and contact pressure have considerable impact on the friction coefficient. Many researchers [7, 8, 11, 13, 29–31] have contributed to the development of the relationship between friction coefficient and temperature, contact pressure. The function of the brakes is to decelerate and stop the vehicle and in doing so it converts the kinetic energy of vehicle

into heat. Figure 5(a) shows how friction coefficient is reduced at high temperatures hence brakes become less efficient and fading also occurs [26].

It can be interpreted that at high contact pressure there is an increasing friction coefficient shown in Fig. 5(b) and this phenomenon can be attributed to the thermomechanical loading. The brake pad materials showed increase in the friction coefficients (5%–19%) with an increasing pressure [30]. It was observed that the contact pressure is affected by the non-linear characteristics of the friction material, and the GAP element parameters such as clearance and contact stiffness are to be adjusted for the friction coefficient [8]. The correlation of the temperature and contact pressure is indicated in the Fig. 5(c). For a constant contact pressure the variations in the temperature and friction coefficient are depicted in Fig. 5(d).

#### 5 Braking system set up

Figure 6 shows the set up of simple dual braking system and Fig. 7 indicate the layout of the set up. The purpose of a dual air brake system is to accommodate a mechanically secured parking brake that can be used during a service brake failure and to accommodate the pipes connecting service reservoir and brake

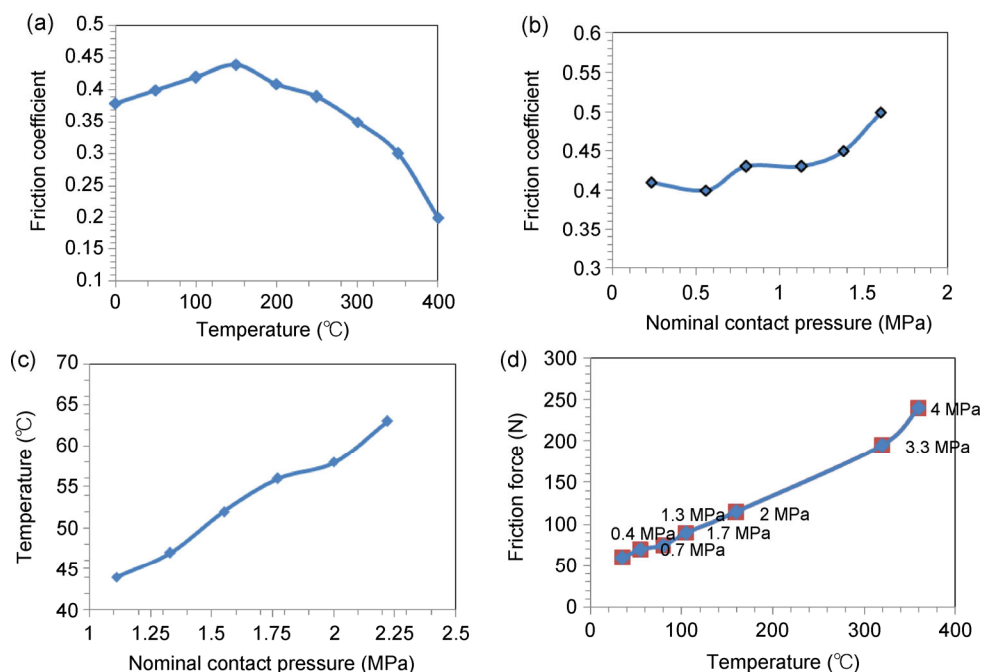


Fig. 5 Correlation of temperature, contact pressure, friction force and friction coefficient.



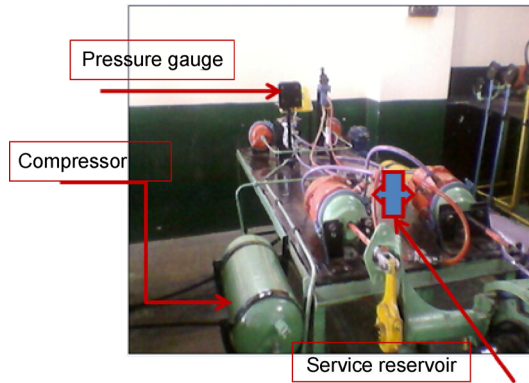


Fig. 6 Braking System set up.

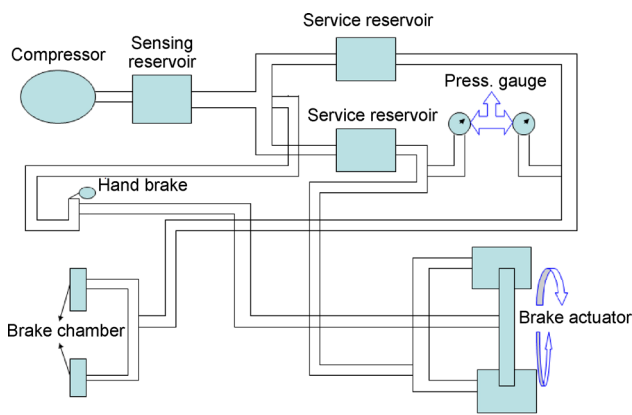


Fig. 7 The layout of braking system set up.

chamber installed with the two pressure gauges as shown in Fig. 7. The brake actuator is connected to the compressor through hand brake and sensing reservoir. Brake chamber is accessing the compressed air through another service reservoir. Service reservoir serves the purpose of safety during the failure. The air compressor is driven by the engine through V-belt.

The test was executed as follows:

- The prestart test ensured enough compressed air in the system to actuate the brake application.
- Air compressor supplied the air pressure of 8 bar for actuating the brakes.
- The set up was actuated to demonstrate working of brake linkage mechanism and to acquire the data regarding operating and geometrical parameters.

From the above steps, a set of data shown in Table 1 was measured under a given operating condition. The measured data was processed with the derived equations earlier to compute the value of friction coefficient ( $\mu$ ).

Table 1 Operating and geometrical parameters.

No.	Parameter	Value
1	$r$	24.3 cm
2	$d$	16 cm
3	$h$	12 cm
4	$W_l, W_t$	24 kgf
5	$m$ (shoe)	0.4 kgf

## 6 Estimation algorithm for computation of the friction coefficient ( $\mu$ )

Brake drum–shoe friction coefficient estimation is vital for estimation of the braking torque, which affects the active safety of the vehicle and the passenger. The estimation algorithm should be of low computational complexity and should present the holistic view of the parameters involved. Figure 8 shows the flowchart for the friction coefficient ( $\mu$ ) estimation. This includes two sub estimators: one is maximum friction coefficient ( $\mu$ ) estimation considering the contact forces when  $F_l$  and  $F_t$  are normal to the contacting surface. The other is for the friction coefficient ( $\mu$ ) estimation using the equations derived for varied conditions of longitudinal forces.

## 7 Simulink modeling

In order to evaluate the performance of the estimation algorithm, it was implemented in the Simulink

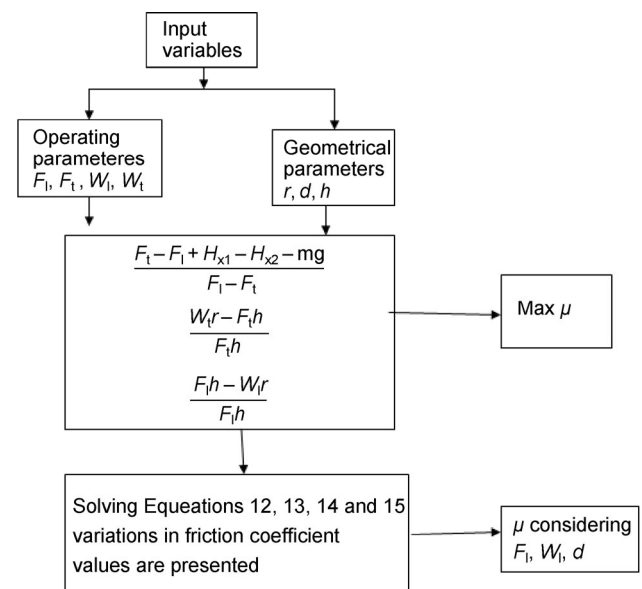


Fig. 8 The Flowchart for friction estimation.

environment with the help of the deduced equations. Simulink modeling has been prepared to illustrate the calculation methodology of the friction coefficient depending on the longitudinal forces used in the formulation of the equations.

Figure 9 depicts the Simulink model for the Eq. (3). The model decomposes the equation in the sequence of mathematical operations. The values for the block parameters varied as variable input from the braking system and geometrical parameters of the referred system. The mathematical operations were processed using the user defined mathematical block functions.

Figure 10 describes the Simulink model for Eq. (5). This computes the friction coefficient ( $\mu$ ) for considering contact force  $F_1$  and actuating force  $W_1$ . The output of the constant blocks was specified by the constant value

parameters obtained from the braking system. Figure 11 shows the Simulink model for Eq. (7). It processed the constant value parameters contact force  $F_v$  and trailing shoe actuating force  $W_1$  and the output denoted by the port 3 resulted in the friction coefficient ( $\mu$ ).

Figure 12 presents the Simulink model for Eq. (12). This comprehensive model estimated the friction coefficient with the inclined arrangement of the contact forces ( $F_1$  and  $F_t$ ) and it has also taken into account the effect of Hinge reactions ( $H_{x1}$  and  $H_{x2}$ ) at the pivot of the brake shoes.

Figure 13 Simulink model for the Eq. (13) estimates the friction coefficient ( $\mu$ ) in the inclined arrangement of the contact forces along with the consideration of the weight component ( $mg$ ) for the brake shoes. The impact of longitudinal force at the trailing shoe and

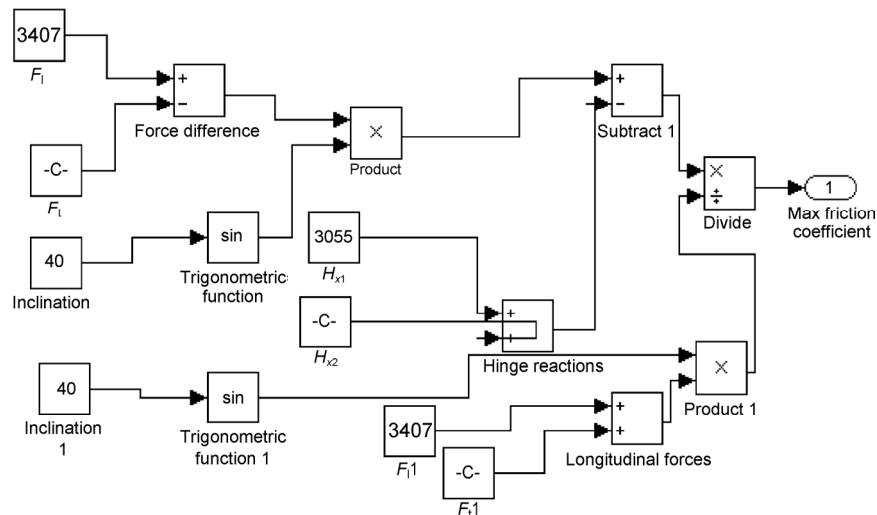


Fig. 9 Simulink model for max friction coefficient estimation.

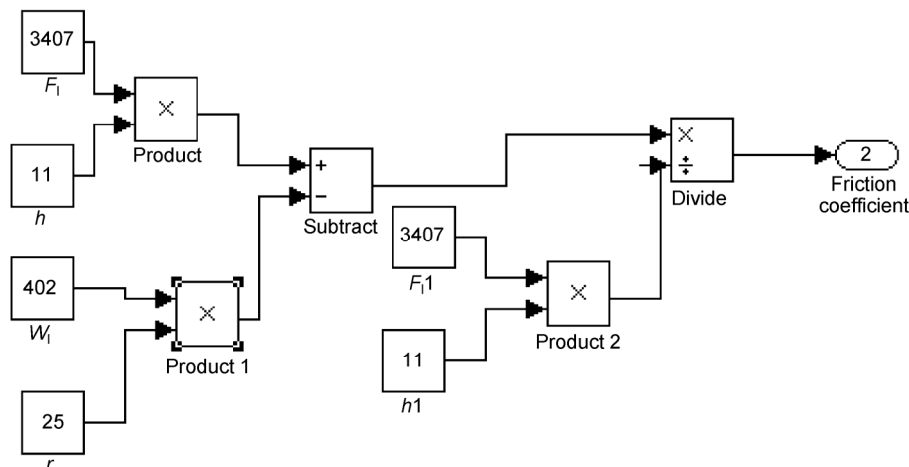


Fig. 10 Simulink model considering leading shoe force.

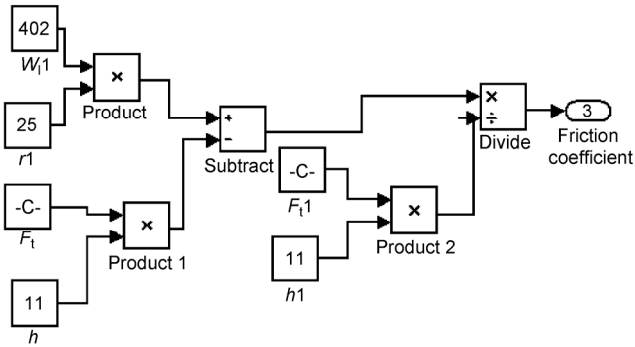


Fig. 11 Simulink model considering  $F_t$  and  $W_1$ .

the brake actuating force reflected in Eq. 15 is shown in the Fig. 14. The values of the constant are varied in the block parameters, and the port 7 estimates the friction coefficient. The decomposed Simulink model shown in Fig. 15 represents the Eq. (14) and port 5

calculates the friction coefficient with the effect of the contact force.

## 8 Development of Simulink model for the braking system

The model presented in the Fig. 16 simulates the dynamics at the brake drum–shoe interface during the braking process. The model presents a single wheel brake which can be replicated a number of times to represent a model for multi wheel vehicle. The brake drums at initial velocity corresponding to the vehicle speed before the brakes are applied. The available data slip between the vehicle speed and drum speed is fixed at 0.8 represented by the constant block parameter. In the present work bang-bang controller is used based upon the actual slip and the desired slip. The control of

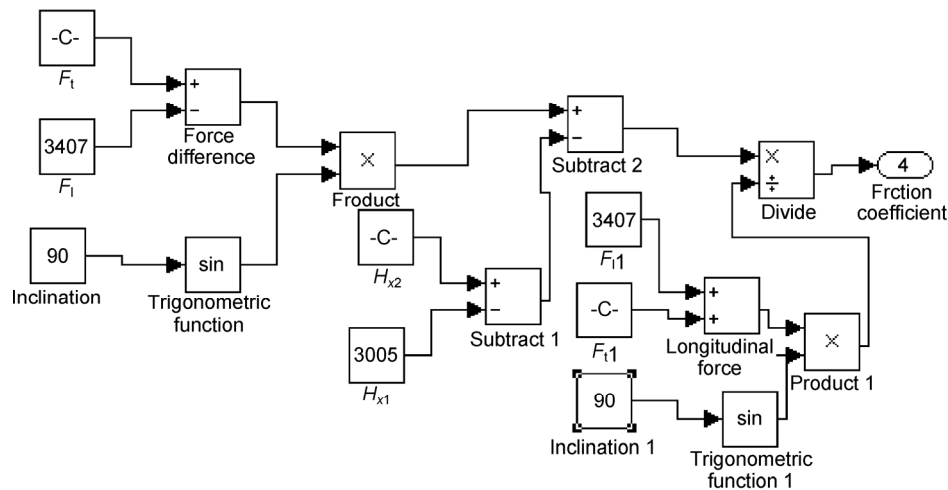


Fig. 12 Simulink model considering  $F_1$ ,  $F_{t1}$  and hinge reactions.

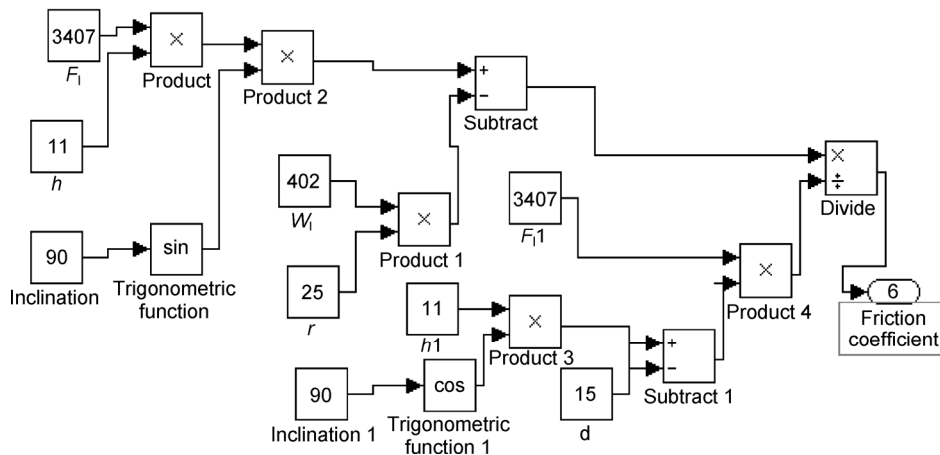


Fig. 13 Simulink model for fland  $W_1$ .



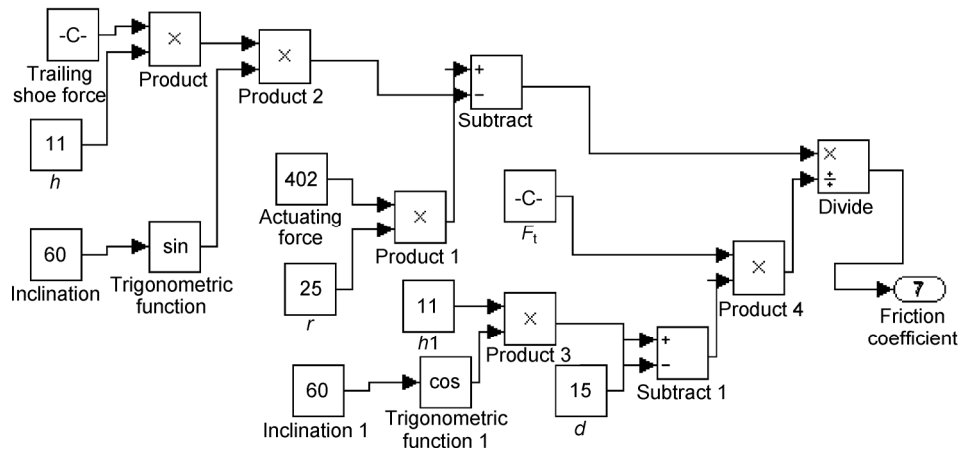


Fig. 14 Simulink model considering  $F_t$  and  $W_t$ .

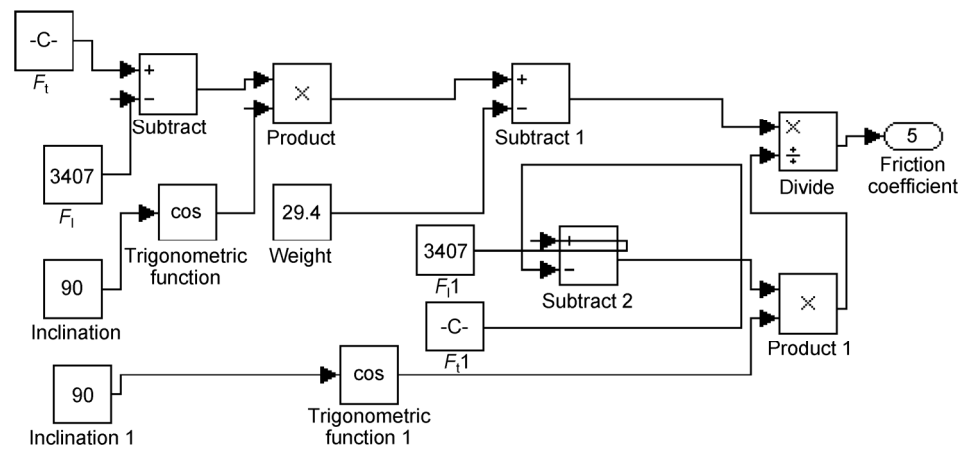


Fig. 15 Simulink model considering  $F_t$  and  $F_t$ .

the brake pressure is considered through a first order lag that represents the delay associated with the hydraulic lines of the brake system. The model then integrates the filtered rate to yield the actual brake pressure. The gain factor for the contact force is fixed at the 1. The calculated brake torque from the contact force and the distance at the shoe–drum interface is set as the block parameter. Further the friction coefficient is obtained by ratio of the forces.

## 9 Validation

The validation of the proposed methods is based on comparison between estimated friction coefficient with the help of output from the deduced equations solved by using the acquired data from set up and friction coefficient resulted from Simulink model of the braking system. The friction coefficient values

between 0.3–0.7 as selected from the database of the simulated results are pertaining in the range proposed by Mortimer and Campbell in 1970 [22] in the earlier work for man–vehicle interface while present study concentrates on brake shoes–drum interface. The operating parameters were obtained from the test runs of the braking trainer set up.

The estimation model presented by Barecki and Scieszka [23] describing the braking system as a kinematic pair of friction computes the friction coefficient considering resultant force and contact force correlating with the present study. The computation of disc–pad coefficient by Fernandez [24] pertains in the 0.25–0.5 similar to demonstrated in the present study for brake shoe–drum interface. Kapoor et al. [25] reported the non-linear relationship between frictional torque and friction coefficient corresponding similar in present study.

## 10 Results and discussion

The database of estimated friction coefficient obtained from the simulation results of the equations are discussed below, depicting a comparison between the friction coefficient ( $\mu$ ) obtained for increasing and decreasing levels of contact, actuating and Coulomb friction forces.

### 10.1 Contact force ( $F_f$ )

Figures 17(a) and 17(b) shows the output produced by the decomposed Simulink Models from the equations obtained for the friction coefficient and variations in the contact force at the leading shoe. The operating parameters acquired while conducting the test runs

were also processed in the Simulink models. The adopted procedure allowed discarding the friction coefficient values adversely affecting the braking maneuver. It has been noticed that the obtained value for friction coefficient ( $\mu$ ) is maximum as compared to the norms [2]. Figures 17(a) and 17(b) show the variations in the friction coefficient ( $\mu$ ) for increasing and decreasing levels of contact forces respectively. The values obtained for the friction coefficient obtained after simulating the Eq. (13) pertains in the acceptable range of 0.4–0.6. The equation expressing relationship of the friction coefficient ( $\mu$ ) with longitudinal forces has been simulated, and the impact of the contact force enables computation of the friction coefficient in the acceptable range 0.4–0.6. Equation 5 obtained

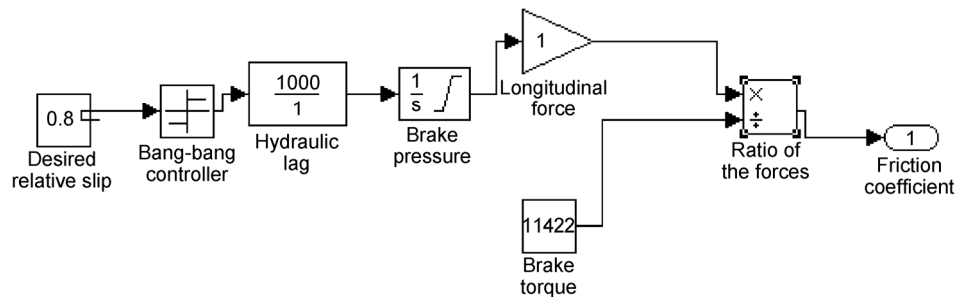


Fig. 16 Simulink model for single wheel drum brake.

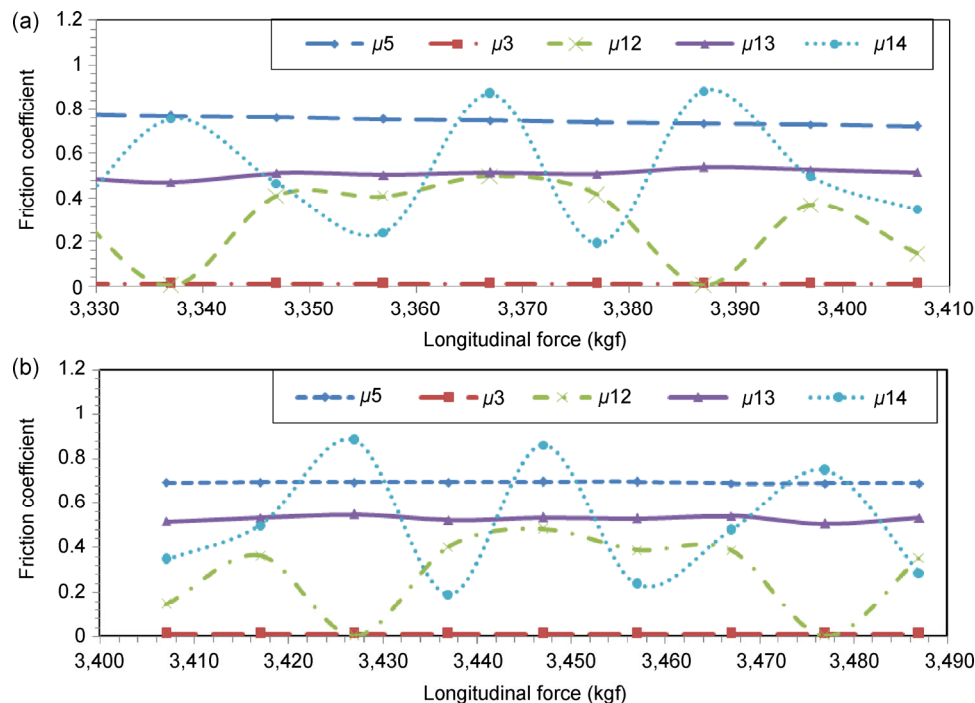


Fig. 17 Friction coefficient variation with contact force.

for the maximum friction coefficient produced the average value of 0.718. This result is adequately high from the value obtained from the Simulink model indicated in Fig. 20. The friction coefficient ( $\mu$ ) values for 3,420 kgf and 3,480 kgf contact forces shows friction coefficient values in the acceptable range. The estimated friction coefficient ( $\mu$ ) presented by Eq. (13) predicts the accurate values in the range of 0.4–0.6.

## 10.2 Actuating force ( $W_i$ and $W_j$ )

The brake actuating ( $W_i$  and  $W_j$ ) forces exerted by the cam mechanism has been assumed equal. The contact forces at the shoe–drum interface are unequal which are responsible for the variations in the computed values for friction coefficient ( $\mu$ ) which can be tracked in the Figs. 18(a) and 18(b). The increasing and decreasing levels of actuating forces were tested using the Simulink models considering various forces as shown in Figs. 18(a) and 18(b) respectively. For each step of estimation, the algorithm implemented in Simulink models showed the computation of the friction coefficient ( $\mu$ ) for all the variations of the actuating forces. The estimation results presented using Eq. (14)

indicates the relationship between actuating force and friction coefficient ( $\mu$ ). The average friction coefficient ( $\mu$ ) of 0.533 computed from Eq. 15 is within the acceptable limits. It can be noticed that friction coefficient ( $\mu$ ) values for the symmetric shoe length given by Eqs. 5 and 7 differs widely on the contrary for the asymmetric shoe length estimated using Eqs. 14 and 15 prevailing in the acceptable range 0.4–0.6.

## 10.3 Coulomb friction force ( $\mu F_i, \mu F_j$ )

Figures 19(a) and 19(b) show the estimation curves for the variations of the Coulomb friction force, the friction coefficient ( $\mu$ ) for the Eq. 14 and friction coefficient ( $\mu$ ) for the Eq. (15). The aforementioned equations represent the impact of the Coulomb friction force. The distribution of the Coulomb friction forces is evaluated with reference to the actuating distance of Coulomb force ( $d$ ), hence the results are presented in the friction coefficient ( $\mu$ ) verses actuating distance of Coulomb force ( $d$ ). The variations in the actuating distance of Coulomb force ( $d$ ) further leads to variations in the friction coefficient ( $\mu$ ). These variations in the friction coefficient ( $\mu$ ) can be attributed to the

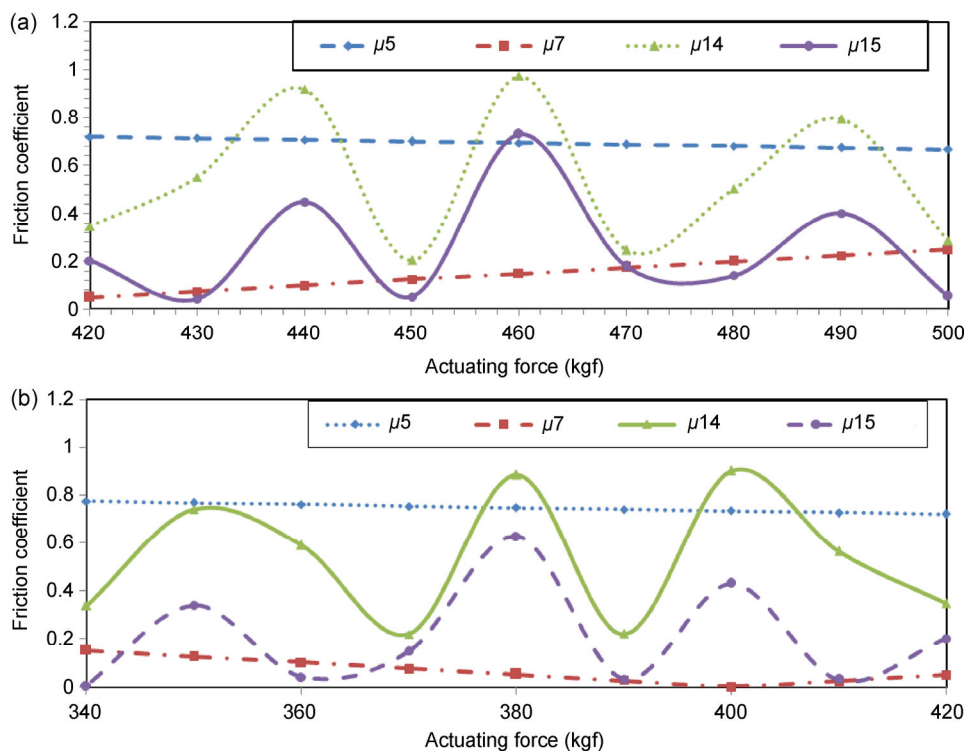


**Fig. 18** Friction coefficient variation with actuating force.

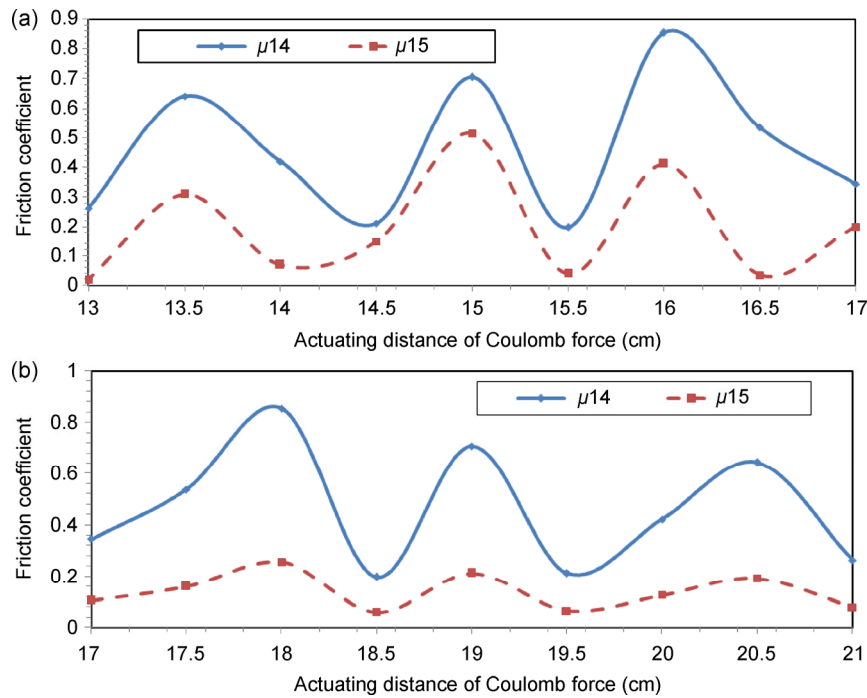


**Fig. 19** Friction coefficient variation with Coulomb force.

statement of the Coulomb friction force that is proportional to the normal reaction.

Considering the Coulomb friction forces ( $\mu F_1$  and  $\mu F_t$ ) as indicated in the Figs. 19(a) and 19(b) shows the average friction coefficient ( $\mu$ ) of 0.464 which is having the error of 6% with the friction coefficient ( $\mu$ ) produced by the Simulink model for the braking system as shown in Fig. 20. It gives the optimum value of 15 cm for the actuating distance of Coulomb friction force. The results of the simulated data considering contact force, actuating force and the Coulomb friction force show fair agreement with friction coefficient ( $\mu$ ) produced by the virtual braking model as shown in Fig. 20.

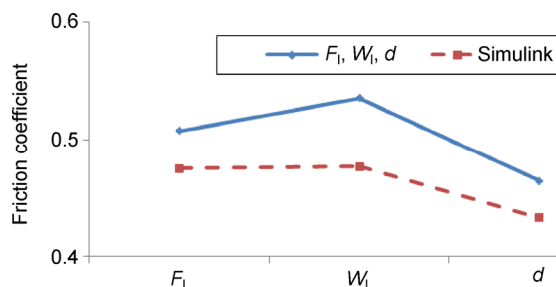


**Fig. 20** Comparison of friction coefficient from equations and simulink brake model.

## 11 Conclusions

The paper presents an effective assessment of the braking system drum–shoe friction coefficient ( $\mu$ ) considering longitudinal forces involved in the braking process using the set of basic equations of classical mechanics with friction. The relationship of influential factors—contact forces ( $F_1$  and  $F_t$ ), actuating force ( $W_1$  and  $W_t$ ) and Coulomb friction forces ( $\mu F_v$  and  $\mu F_t$ ) with friction coefficient ( $\mu$ ) was used in the estimation algorithm to compute the friction coefficient ( $\mu$ ).

- The maximum friction coefficient ( $\mu$ ) 0.7 obtained for symmetric shoe length considering abovementioned influential factors indicated in Figs. 17(a) and 17(b), while for asymmetric shoe length it varies between 0.3–0.7.
- According to the simulation results it can be asserted that the Coulomb friction force ( $\mu F_1$  and  $\mu F_t$ ) is dependent on the contact force ( $F_1$  and  $F_t$ ) and brake actuating force ( $W_1$  and  $W_t$ ) and this also can be interpreted from the output of the Eqs. 3, 5 and 12–14 for symmetric as well as for the asymmetric shoe length.
- The parameter identification and state estimation method presented in the paper can accurately

predict the state of the braking system and drum–shoe interface friction coefficient ( $\mu$ ) which will achieve desired safety control and is also useful for automobile brake designers for preparing ABS algorithm and computing accurate brake torque.

- In this paper longitudinal dynamics are used to design the friction estimation algorithm processed by the Simulink models. The lateral dynamics can be considered for friction coefficient ( $\mu$ ) in the future.

## Nomenclature

- $\mu$ : Friction coefficient.  
 $F_l$ : Longitudinal contact force for leading shoe (Kgf).  
 $F_t$ : Longitudinal contact force for trailing shoe (Kgf).  
 $W_l$ : Actuating forces for leading and trailing shoes (Kgf).  
 $W_t$ : Actuating forces for leading and trailing shoes (Kgf).  
 $H_{x1}, H_{x2}$ : Hinge reaction in  $x$  direction (Kgf).  
 $mg$ : Weight component of the brake shoes.  
 $\theta$ : Angle of the longitudinal force with vertical ( $^\circ$ ).  
 $h$ : Distance between the centre of the pivot and centre of the drum (cm).  
 $r$ : Distance between the centre of the pivot and inclined force (cm).  
 $d$ : Distance between the centre of the pivot and Coulomb force (cm).  
 $\mu F_l$ : Coulomb friction force for leading shoe.  
 $\mu F_t$ : Coulomb friction force for trailing shoe.

**Open Access:** This article is distributed under the terms of the Creative Commons Attribution License which permits any use, distribution, and reproduction in any medium, provided the original author(s) and source are credited.

## References

- [1] Giri N K. *Automotive Mechanics*. New Delhi (India): Khanna Publisher, 1990.
- [2] Mortimer R G, Campbell J D. Brake force requirement study: Driver-vehicle braking performances a function of brake system design variables. Highway Safety Research Institute, 1970: 1–222.
- [3] Blau P J. *Compositions, Functions, and Testing of Friction Brake Materials and Their Additives*. Oak Ridge National Laboratory, ORNL/TM-2001/64:1–38, 2001.
- [4] Li Z, Peng X, Xiang X, Zhu S-H. Tribological characteristics of C/C-SiC braking composites under dry and wet conditions. *T Nonferr Mater Soc* **18**: 1071–1075 (2008)
- [5] Maleque M A, Dyuti S, Rahman M M. Material selection method in design of automotive brake disc. In *Proceedings of the World Congress on Engineering*, London, Vol III, 2010: 1–5.
- [6] Abu Bakar A R, Ouyang H. Prediction of disc brake contact pressure distributions by finite element analysis. *Jurnal Teknologi* **43**: 21–36 (2005)
- [7] Hohmann C, Schiner K, Oerter K, Reese H. Contact analysis for drum brakes and disk brakes using ADINA. *Comput Struct* **72**: 185–198 (1999)
- [8] Junzo T, Kazuhiro D, Tadashi T. Prediction of contact pressure of disc brake pad. *Technical Notes/JSAE Rev* **21**: 133–141 (2000)
- [9] Burton R A, Kilaparti S R, Nerlikar V. A limiting stationary configuration with partially contacting surfaces. *Wear* **24**: 199–206 (1973)
- [10] Cueva G, Sinatora A, Guesser W L, Tschiptschin A P. Wear resistance of cast irons used in brake disc rotors. *Wear* **255**: 1256–1260 (2003)
- [11] Guha D, Roy Choudhary S K. Effect of surface roughness on temperature at the contact between sliding bodies. *Wear* **197**: 63–73 (1996)
- [12] Li J, Zha X, Wu D. The theoretical analysis of test result's errors for the roller type automobile brake tester. *Int Fed Info Proc* **347**: 382–389 (2011)
- [13] Yasuhisa A. Lowering friction coefficient under low loads by minimizing effects of adhesion force and viscous resistance. *Wear* **254**: 965–973 (2003)
- [14] Severin D, Dorsch S. Friction mechanism in industrial brakes. *Wear* **249**: 771–779 (2001)
- [15] Berger E J. Friction modeling for dynamic system simulation. *ASME* **55**: 535–577 (2002)
- [16] Kowalski W, Skorupka Z, Kajka R, Amborski J. Car brake system analytical analysis. In *Proceedings 24th European Conference on Modelling and Simulation*.
- [17] Vazquez Alvarez I, Ocampo-Hidalgo J J, Ferreyra-Ramírez A C, Avil'es-Cruz C. Mathematical model for automobile's braking process considering a friction coefficient dependent of the longitudinal velocity. In *Proceedings of the 15th WSEAS International Conference on Systems*, 2011: 185–189.
- [18] Rabia A M, Ghazaly N M, Salem M M, Abd-El-Tawwab A M. Experimental Studies of Automotive Disc Brake Noise and Vibration: A Review. *Int J Mod Eng Res (IJMER)* **3**: 199–203 (2013)
- [19] Delaigue P, Eskandarian A. A comprehensive vehicle braking

- model for predictions of stopping distances. *J Automob Eng* **218**: 1411–1413 (2004)
- [20] Jean-Philippe D, Christophe P, Thierry S, Sophie C. Comparison of several methods for real pedestrian accident reconstruction. In *Proceedings of the 19th International Technical Conference on the Enhanced Safety of Vehicles (ESV)*, 2001: 1–14.
- [21] Ostermeyer G P. on the dynamics of the friction coefficient. *Wear* **254**: 852–858 (2003)
- [22] Vista B. Brake Bible Pirtes 4x4.com Braking on soft sensing technique. *J Phys*: 730–733 (2008)
- [23] Barecki Z, Scieszka S F. A mathematical model of brake shoe and the brake path system. *N&O Joernaal*: 13–17 (1987)
- [24] Fernandez J G. *A Vehicle Dynamics Model for Driving Simulators*. Chalmers University, Sweden, 2012.
- [25] Kapoor A, Tung S C, Schwartz S E, Priest M, Dwyer-Joyce R S. *Automotive Tribology*. CRC Press LLC, 2001.
- [26] Fowler A C. *Techniques of Applied Mathematics*. Mathematical Institute, Oxford University, 2005.
- [27] Thomas B. *Modeling of Mechanical Systems*. Lecture Notes Aalborg University of Technology, 2002: 1–77.
- [28] Nobrant P. *Driveline Modelling Using Math Modelica*. Linkopings Institute, 2001.
- [29] Liew K W, Nirmal U. Frictional performance evaluation of newly designed brake pad materials. *Mater Design* **48**: 25–33 (2013)
- [30] Ali B, Mostefa B. Thermal behaviour of dry contacts in the disc brakes. *Int J Automot Eng* **3**: 9–17 (2012)
- [31] Osterle W, Urban I. Friction layers and friction films on PMC brake pads. *Wear* **257**: 215–226 (2004)



**Hrishikesh P. KHAIRNAR.** He is a research scholar and faculty at VJTI. He received his master degree in engineering at VJTI in 2005 and joined VJTI as faculty in 2008. His

teaching experience encapsulates subjects of automotive power transmission systems and mechatronics. Currently he is a doctor candidate in the area of “friction modeling of automotive brakes” since 2012 in quest to improve automotive safety.



**Vikas M. PHALLE.** He obtained his ME degree from VJTI in 2004 and Ph.D degree at IIT Roorkee in 2011 pertaining to the area “performance analysis of fluid film journal bearing”. He has 20 years teaching experience and his research work

has been recognized at international level with more than 45 research papers in reputed and high impact factor international and national Journals. He is also the reviewer of many international peer review journals. Recently he presented paper at STLE Annual Meeting at Dallas, USA, 2015.



**Shankar S. MANTHA.** He is an eminent academician and an able administrator. He obtained his ME degree at VJTI. His Ph.D research pertained to the area of “combustion modeling”. His passion for developing the IT solutions for the transparency in government and speedy approval process vindicated in the projects for the state of

Maharashtra, and Municipal Corporations. His stint at All India Council for Technical education (Country’s leading regulatory body for engineering colleges) since March 2009 as Vice-Chairman and August 2009 as Chairman was an attempt to expedite the process of approvals and enabling accountability. He has more than 175 publications in international journals and conferences to his credit and 12 Ph.D students who have completed their Ph.D research.